Journal of *Marine Science and Engineering*

MDPI

Article

Numerical Analysis of Sandwich Composite Deep Submarine Pressure Hull Considering Failure Criteria

Mahmoud Helal [1,2,3,4], Huinan Huang [1,2], Defu Wang [1,2,*] and Elsayed Fathallah [1,2,5,*]

1 College of Engineering, Northeast Agricultural University, Harbin 150030, China; Eng_mah_helal@yahoo.com (M.H.); huinanhuang0312@163.com (H.H.)
2 Key Laboratory of Swine Facilities Engineering, Ministry of Agriculture, Harbin 150030, China
3 Department of Mechanical Engineering, Faculty of Engineering, Taif University, Taif 21974, Saudi Arabia
4 Production and Mechanical Design Dept., Faculty of Engineering, Mansoura University, Mansoura 35516, Egypt
5 Department of Civil Engineering, Military Technical College, Kobry Elkobba, Cairo 11865, Egypt
* Correspondence: dfwang0203@163.com (D.W.); saidhabib2000@hotmail.com (E.F.)

Received: 2 October 2019; Accepted: 19 October 2019; Published: 22 October 2019

Abstract: The pressure hull is the primary element of submarine, which withstands diving pressure and provides essential capacity for electronic systems and buoyancy. This study presents a numerical analysis and design optimization of sandwich composite deep submarine pressure hull using finite element modeling technique. This study aims to minimize buoyancy factor and maximize deck area and buckling strength factors. The collapse depth is taken as a base in the pressure hull design. The pressure hull has been analyzed using two composite materials, T700/Epoxy and B(4)5505/Epoxy, to form the upper and lower faces of the sandwich composite deep submarine pressure hull. The laminated control surface is optimized for the first ply failure index (*FI*) considering both Tsai–Wu and maximum stress failure criteria. The results obtained emphasize an important fact that the presence of core layer in sandwich composite pressure hull is not always more efficient. The use of sandwich in the design of composite deep submarine pressure hull at extreme depths is not a safe option. Additionally, the core thickness plays a minor role in the design of composite deep submarine pressure hull. The outcome of an optimization at extreme depths illustrates that the upper and lower faces become thicker and the core thickness becomes thinner. However, at shallow-to-moderate depths, it is recommended to use sandwich composite with a thick core to resist the shell buckling of composite submarine pressure hull.

Keywords: multi-objective optimization; sandwich composite; buoyancy factor; Tsai–Wu; failure criteria

1. Introduction

Optimization plays an important role in obtaining the best composite hull with high efficiency and safe use of materials. Most submarine designs are weight critical, especially when the operational diving depth increases. Therefore, the designers will strive to select an available high strength and low-density material. Diving depth is an essential criterion for designing a submarine pressure hull for a certain collapse depth at which failure must be expected within a narrowly limited range of tolerance [1]. Working at depths of several kilometers requires perception of how hydrostatic pressure affects both structures and materials [2]. Changing the hull weight allows the vessel to submerge and change depth in a controlled manner. A submarine is not allowed to go further than the service diving depth [3,4]. At great depths, composite materials are the only solution available. The design and analysis of composite structures are more complicated than metallic structures, through

layer stacking sequence, orientation, and number of plies used for manufacturing of laminates [5]. Significant research work has been presented so far in that field. Among that research, Mian et al. [6] optimized a composite pressure vessel, taking into account both Tsai–Wu and maximum stress failure criteria. Helal et al. [7] optimized a pressure hull to increase the payload, after that, underwater explosions (UNDEX) were investigated. Also, Pan et al. [8] investigated the design optimization of composite shell subjected to hydrostatic pressure. The thickness and the layer orientation were studied using the distribution optimization method. Zhang et al. [9] applied the multidisciplinary design optimization method to design a new underwater vehicle. Furthermore, Pelletier and Vel [10] presented a multi-objective design optimization methodology for a laminate composite materials. The fiber volume fractions and orientations were chosen as the elementary optimization variables. Lund [11] optimized laminated composite structures using failure criteria. Likewise, Fathallah et al. [12–15] investigated the optimization of composite pressure hull for both maximizing the buckling load capacity and minimizing the buoyancy factor. Also, Panteleev [16] optimized sandwich structures and assured a reduction in their weight of 23% compared with the constant thickness plate. On the other hand, Garland [17] illustrated a higher strength material and stiffness provided better buoyancy and less weight. Messager et al. [18] presented the optimum design of autonomous underwater vehicles. Furthermore, they investigated the optimal lamination design of an un-stiffened thin composite underwater vessels subjected to buckling. Ca et al. [19] investigated the composite pressure vessel subjected to an external pressure. The results illustrated that, when the applied load was bigger than the critical buckling load, buckling and burst behaviors were occurred. In addition, Lee et al. [20] optimized the composite cylinder under hydrostatic pressure incorporating both the material failure and buckling. Smith et al. [21] described an advanced integrated approach to structural modeling analysis and design of underwater vehicles. Also, Sekulski [22] presented a multi-objective optimization of high speed vehicle passenger catamaran structure. The strength criteria were taken from the adopted classification rules. Furthermore, Aly et al. [23] presented a design optimization procedure of a sandwich panels for material selection and sizing as an alternative to the normal panels. On the other hand, Walker and Smith [24] presented a multi-objective optimization of a composite structures for minimizing both weight and deflection. Likewise et al. [25], presented an optimization methodology to minimize the mass of composite plates subjected to an in-plane loading. Additionally, Bakshi and Chakravorty [26] maximized the failure load of thin composite conoidal shells using first layer failure. Kalantari et al. [27] investigated the multi-objective optimization of T700Scarbon/S-2 glass fiber-reinforced epoxy hybrid composites to minimize the weight and cost of laminates. The fiber type, orientation angle, and volume fraction in each lamina were considered as the design variables. Also, Liang et al. [28] optimized a multiple intersecting spheres pressure hull for minimizing the buoyancy factor. Kim et al. [29] maximized the strength and the failure index of Tsai–Hill criterion for a composite wing. MacKay et al. [30] investigated the corrosion effect on stability and strength of pressure hulls. The results showed that there was a reduction in the overall collapse and yield pressure about 20% and 40%, respectively. Zhang et al. [31] investigated the egg-shaped pressure hulls effect on enhancing the hydrodynamics of spherical pressure hulls, buckling resistance, and interior arrangements. On the other hand, Song et al. [32] optimized a composite cylindrical hull to minimize the hull structural weight using multi island genetic algorithm. Also, Carpentieri and Skelton [33] designed a composite structure composed of composite membranes and cable networks to minimize the structural weight. While, Ren et al. [34] predicted the buckling behavior and stress condition of a composite cylindrical pressure hull using finite element analysis. Also, Rao and Lakshmi [35] presented a mimetic algorithm for combinatorial optimization of laminate composite structures. The results revealed that the buckling strength of boron epoxy is four times higher than glass epoxy. Zhu et al. [36] studied the buckling behaviors of a spherical shell with an opening. The critical load with an opening was about 4.4–8% lower than that of the complete spherical shell. Ross and Little [37] predicted the buckling pressure of a carbon fiber vessel subjected to an external pressure. It was observed that the experimental results were 20% higher than FE prediction. Lopatin and Morozov [38] presented an analytical solution for

the buckling problem of a composite cylindrical subjected to hydrostatic pressure. The maximum critical pressure was achieved when the helical angle equaled 65°. The value of the critical load can be increased 15% with varying the helical angle. Aydogdu and Aksencer [39], studied the buckling of composite plates considering the linear variation in planeloads and different plate theories. Likewise, Han et al. [40], studied the buckling and post-buckling behavior of composite cylindrical shells under external pressure. Also, Vosoughi et al. [41] obtained the optimum fibers orientation of thick composite plate layers for maximizing the buckling load. Erdal and Sonmez [42] presented a design procedure for maximizing the load that the composite laminate can sustain without buckling.

In this work, a multi-objective optimization methodology for non-circular cross-section pressure hull, as illustrated in Figure 1, is presented. T700/epoxy and B(4)5505/Epoxy composites have promise for these applications according to [12]. T700/Epoxy is used at extreme depths while B(4)5505/Epoxy is used at shallow-to-moderate depths. Maximizing the deck area and minimizing the buoyancy factor (the weight/displacement ratio) of the pressure hull subjected to external hydrostatic pressure at maximum operating depth are considered the objective functions of using T700/Epoxy as face sheets. Also, maximizing the buckling load capacity and minimizing the buoyancy factor are considered the objective functions at low to moderate depths using B(4)5505/Epoxy as face sheets.

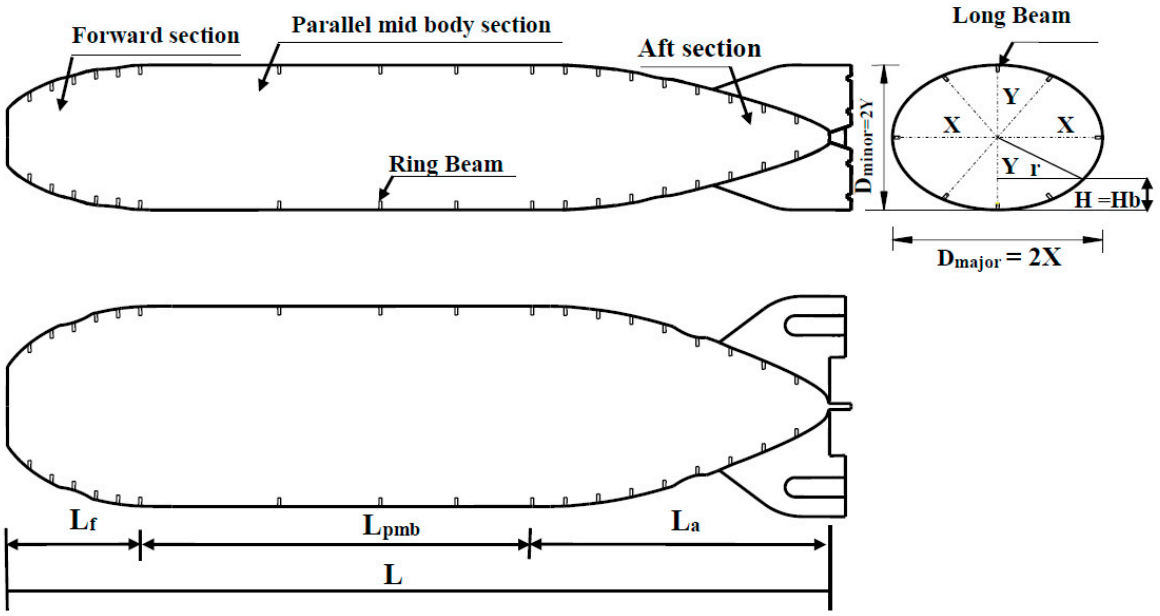

Figure 1. Parameterization of non-circular submersible pressure hulls.

2. Buckling in Composite Pressure Hull

Multilayer composite pressure hulls are buckle when the actual load exceeds its critical value. To ensure stability, the critical buckling strength (N_{cr}) must exceed the actual load (N_{act}). The buckling strength factor (λ) is introduced to identify the buckling of pressure hulls and expressed as presented in Equation (1)

$$\lambda = \frac{N_{cr}}{N_{act}} \tag{1}$$

In the buckling assessment, the linear buckling is considered. Buckling occurs when P_{cr} and N_{cr} is less than one ($\lambda < 1$). The critical buckling pressure is the minimum value of P_{cr} and N_{cr} as shown in Equations (2) and (3) [43,44]

$$P_{cr} = \left(\frac{L}{(m\pi)}\right)^2 \frac{\begin{bmatrix} C_{11} & C_{12} & C_{13} \\ C_{21} & C_{22} & C_{23} \\ C_{31} & C_{32} & C_{33} \end{bmatrix}}{\begin{bmatrix} C_{11} & C_{12} \\ C_{21} & C_{22} \end{bmatrix}} \tag{2}$$

$$N_{cr} = \left(\frac{R}{(n^2)}\right) \frac{\begin{bmatrix} C_{11} & C_{12} & C_{13} \\ C_{21} & C_{22} & C_{23} \\ C_{31} & C_{32} & C_{33} \end{bmatrix}}{\begin{bmatrix} C_{11} & C_{12} \\ C_{21} & C_{22} \end{bmatrix}} \tag{3}$$

where L represents the length, R represents the radius, m and n are the number of buckle half waves in the axial and circumferential direction, respectively. Moreover, C, A, B and D are expressed in Equation (4) as

$$\begin{aligned}
C_{11} &= A_{11}\left(\tfrac{m\pi}{L}\right)^2 + A_{66}\left(\tfrac{n}{R}\right)^2 \\
C_{22} &= A_{22}\left(\tfrac{n}{R}\right)^2 + A_{66}\left(\tfrac{m\pi}{L}\right)^2 \\
C_{33} &= D_{11}\left(\tfrac{m\pi}{L}\right)^4 + (4D_{66} + 2D_{12})\left(\tfrac{m\pi}{L}\right)^2\left(\tfrac{n}{R}\right)^2 + D_{22}\left(\tfrac{n}{R}\right)^4 \\
&+ \tfrac{A_{22}}{R^2} + 2\tfrac{B_{22}}{R^2}\left(\tfrac{n}{R}\right)^2 + 2\tfrac{B_{12}}{R^2}\left(\tfrac{m\pi}{L}\right)^2 \\
C_{12} &= C_{21} = (A_{12} + A_{66})\left(\tfrac{m\pi}{L}\right)\left(\tfrac{n}{R}\right) \\
C_{23} &= C_{32} = (B_{12} + 2B_{66})\left(\tfrac{m\pi}{L}\right)^2\left(\tfrac{n}{R}\right) + \tfrac{A_{22}}{R}\left(\tfrac{n}{R}\right) + B_{22}\left(\tfrac{n}{R}\right)^3 \\
C_{13} &= C_{31} = \tfrac{A_{12}}{R}\left(\tfrac{m\pi}{L}\right) + B_{11}\left(\tfrac{m\pi}{L}\right)^3 + (B_{12} + 2B_{66})\left(\tfrac{m\pi}{L}\right)\left(\tfrac{n}{R}\right)^2
\end{aligned} \tag{4}$$

where A_{ij}, B_{ij} and D_{ij} denote the extensional stiffness, coupling stiffness and bending stiffness coefficient matrix, respectively and are defined as expressed in Equation (5)

$$\begin{aligned}
A_{ij} &= \sum_{k=1}^{n} (\overline{Q}_{ij})_k (Z_k - Z_{k-1}), \\
B_{ij} &= \tfrac{1}{2}\sum_{k=1}^{n} (\overline{Q}_{ij})_k (Z_k^2 - Z_{k-1}^2), \\
D_{ij} &= \tfrac{1}{3}\sum_{k=1}^{n} (\overline{Q}_{ij})_k (Z_k^3 - Z_{k-1}^3)
\end{aligned} \tag{5}$$

where n is the number of different plies in the stacking sequence and Z_k, Z_{k-1} denote the upper and lower (Z) coordinate of the k_{th} layer. $\overline{Q}_{ij}$ are the elements of the transformed reduced stiffness matrix $\left[\overline{Q}\right]$ and are defined as presented by [45] in Equation (6)

$$\begin{aligned}
\overline{Q}_{11} &= Q_{11}m^4 + 2(Q_{12} + 2Q_{66})n^2m^2 + Q_{22}n^4 \\
\overline{Q}_{22} &= Q_{11}n^4 + 2(Q_{12} + 2Q_{66})n^2m^2 + Q_{22}m^4 \\
\overline{Q}_{12} &= (Q_{11} + Q_{22} - 4Q_{66})n^2m^2 + Q_{12}\left(m^4 + n^4\right) \\
\overline{Q}_{16} &= (Q_{11} - Q_{12} - 2Q_{66})m^3n + (Q_{12} - Q_{22} + 2Q_{66})n^3m \\
\overline{Q}_{26} &= (Q_{11} - Q_{12} - 2Q_{66})mn^3 + (Q_{12} - Q_{22} + 2Q_{66})m^3n \\
\overline{Q}_{66} &= (Q_{11} + Q_{22} - 2Q_{12} - 2Q_{66})m^2n^2 + Q_{66}\left(n^4 + m^4\right)
\end{aligned} \tag{6}$$

where $m = \cos\theta, n = \sin\theta, \theta_k$ is the orientation angle of the k_{th} layer and Q_{ij} are the plane stress-reduced stiffness for the k_{th} lamina and can be defined in terms of elastic properties of material (E_1, E_2, G_{12}, v_{12} and v_{21}) as mentioned in Equation (7)

$$\begin{aligned} Q_{11} &= (1-\upsilon_{12}\upsilon_{21})^{-1}E_1, \\ Q_{12} &= (1-\upsilon_{12}\upsilon_{21})^{-1}E_1\upsilon_{21}, \\ Q_{22} &= (1-\upsilon_{12}\upsilon_{21})^{-1}E_2, \\ Q_{66} &= G_{12} \end{aligned} \tag{7}$$

For structures exposed to hydrostatic pressure, the effect of buckling should be taken into consideration. The structural stability requirement to be achieved when (N_{cr}) is greater than the design pressure (N_d) [46].

3. Composite Failure Criteria

The successful design requires an efficient and safe use of materials. Therefore, theories are needed to develop and compare the state of stresses and strains in materials [47].

3.1. Maximum Stress Failure Theory

The failure index is presented in Equation (8) [48]

$$FI = \max\begin{cases} \sigma_{11}/X_t \text{ if } \sigma_{11} > 0 \text{ or } -\sigma_{11}/X_c \text{ if } \sigma_{11} < 0 \\ \sigma_{22}/Y_t \text{ if } \sigma_{22} > 0 \text{ or } -\sigma_{22}/Y_c \text{ if } \sigma_{22} < 0 \\ |\tau_{12}|/S \end{cases} \tag{8}$$

where: σ_{11}, σ_{22} and τ_{12} denote the longitudinal, transversal and shear stresses components, respectively, obtained using Equation (9)

$$\begin{Bmatrix} \sigma_{11} \\ \sigma_{22} \\ \tau_{12} \end{Bmatrix} = \begin{bmatrix} Q_{11} & Q_{12} & 0 \\ Q_{12} & Q_{22} & 0 \\ 0 & 0 & Q_{66} \end{bmatrix} \begin{Bmatrix} \varepsilon_{11} \\ \varepsilon_{22} \\ \gamma_{12} \end{Bmatrix} \tag{9}$$

where: X_t, X_c, Y_t, Y_c and S denote the ultimate longitudinal, transversal, and shear strength constants, respectively. Since the sandwich core is considered as an isotropic material, the maximum stress criterion can be used for its failure analysis.

3.2. Tsai–Wu Failure Criteria

The criterion can be expressed as presented in Equation (10) [49,50]

$$FI = \sigma_{11}\left(\frac{1}{X_t} - \frac{1}{X_c}\right) + \sigma_{22}\left(\frac{1}{Y_t} - \frac{1}{Y_c}\right) - \frac{\sigma_{11}^2}{X_t \times X_c} - \frac{\sigma_{22}^2}{Y_t \times Y_c} - \frac{\tau_{12}^2}{S^2} \tag{10}$$

where: X_t, Y_t, X_c, Y_c, σ_{11}, σ_{22} and τ_{21} are aforementioned. FI is the failure index.

The failure occurs when the FI reaches or exceeds one [51].

3.3. Von-Mises Yielding Criteria

The core layer will be modeled with homogenized properties. Therefore, the von Mises yielding criteria is the most appropriate method and employed here to assess the capability of the core material to withstand the yielding failure. The failure index (FI) is defined as in Equation (11) [52]

$$FI = \frac{\sqrt{\sigma_{11}^2 - \sigma_{11}\sigma_{22} + \sigma_{22}^2}}{\sigma_0} \tag{11}$$

where: σ_0 is the material allowable yielding strength, σ_{11} and σ_{22} are the in-plane principal stresses.

4. Deck Area

The internal arrangements of submarines are considered complicated due to the limited space available to accommodate the on-board systems [53]. In this study, it is assumed that maximizing deck area is an achievement from the standpoint of future arrangement execution. Therefore, a simplified analytical model was adopted to calculate the deck area similar to that presented by Vlahopoulos and Hart [54]. The deck height is known as the centerline plane of the submarine. The parametric model is shown in Figure 1, the pressure hull is composed of a non-circular cross-section of total length (L_{tot}) which can be calculated as in Equation (12)

$$L_{tot} = L_{pmb} + L_a + L_f \tag{12}$$

where (L_{pmb}) denotes the parallel mid body length, (L_a) denotes the aft length, and (L_f) denotes the forward length. The goal of the optimization is to maximize the calculated deck area. The adopted equations to calculate the deck area (A_{pmb}) are presented in Equation (13)

$$\begin{aligned} &\tfrac{x^2}{a^2} + \tfrac{y^2}{b^2} = 1 \\ &\tfrac{x^2}{a^2} + \tfrac{(b-h)^2}{b^2} = 1 \\ &x^2 = a^2\left(1 - \tfrac{(b-h)^2}{b^2}\right) \\ &x = r_i = a\sqrt{1 - \left(1 - (\tfrac{b}{h})\right)^2} \\ &A_{deck(pmp)} = 2a\sqrt{1 - \left(1 - (\tfrac{b}{h})\right)^2} \times L_{pmp} \end{aligned} \tag{13}$$

where (r_i) is the half-width of deck in the parallel mid body. The total deck area ($A_{dek\,(tot)}$) can be evaluated according to Equation (14)

$$A_{deck(tot)} = A_{deck(pmb)} + A_{deck(a)} + A_{deck(f)} \tag{14}$$

5. Materials and Methods

The utilized materials for the pressure hulls must be resisting the external pressures and have appropriate properties that can resist the surrounding environment [55]. Composite materials are the best solution for underwater pressure hull and reduce the structural weight [56]. Two candidate composite materials T700/epoxy and B(4)5505/Epoxy are chosen to form the laminates, upper and lower faces, and stiffeners. T700/Epoxy is used at extreme depths which have high stiffness and strength and B(4)5505/Epoxy is used at shallow-to-moderate depths which have high compression strength in order to resist buckling. The low-density PVC foam material is used as a core material. The material properties and the strength parameters of T700/epoxy, B(4)5505/Epoxy composites and PVC foam are demonstrated in Table 1 [57,58]. Figure 2a illustrates the relationship between the collapse depth and buoyancy factor (B.F). While Figure 2b shows some curves of collapse depths versus the weight to displacement ratio in case of material and buckling failures for un-stiffened cylinders constructed from (HY80, GRP, and CFRP) materials [59]. The straight lines correspond to the material failures while the curved lines correspond to the buckling failure.

Table 1. Strengths of unidirectional composites and material properties of sandwich components

Material	Material and Strength Properties
(T700/epoxy composites)	E_{11} = 132 GPa, E_{22} = 10.3 GPa, E_{33} = 10.3 GPa, G_{12} = 6.5 GPa, G_{13} = 6.5 GPa, G_{23} = 3.91 GPa, υ_{12} = 0.25, υ_{13} = 0.25, υ_{23} = 0.38, X_t = 2150 MPa, X_c = 2150 MPa, Y_t = 298 MPa, Y_c = 298 MPa, S = 778 MPa, ρ = 1570 kg/m^3
(B(4)/5505 Boron/Epoxy)	E_{11} = 204 GPa, E_{22} = 18.5 GPa, E_{33} = 18.5 GPa, G_{12} = 5.59 GPa, G_{13} = 5.59 GPa, υ_{12} = 0.23, X_t = 1260 MPa, X_c = 2500 Mpa, Y_t = 61 MPa, Y_c = 202 MPa, S = 67 MPa, ρ = 2000 kg/m^3
(H200 (foam core))	E = 250 MPa, G = 73 MPa, υ = 0.3, X_t = 7.1 MPa, X_c = 5.4 Mpa, Y_t = 7.1 MPa, Y_c = 5.4 MPa, S = 3.5 MPa, ρ = 200 kg/m^3

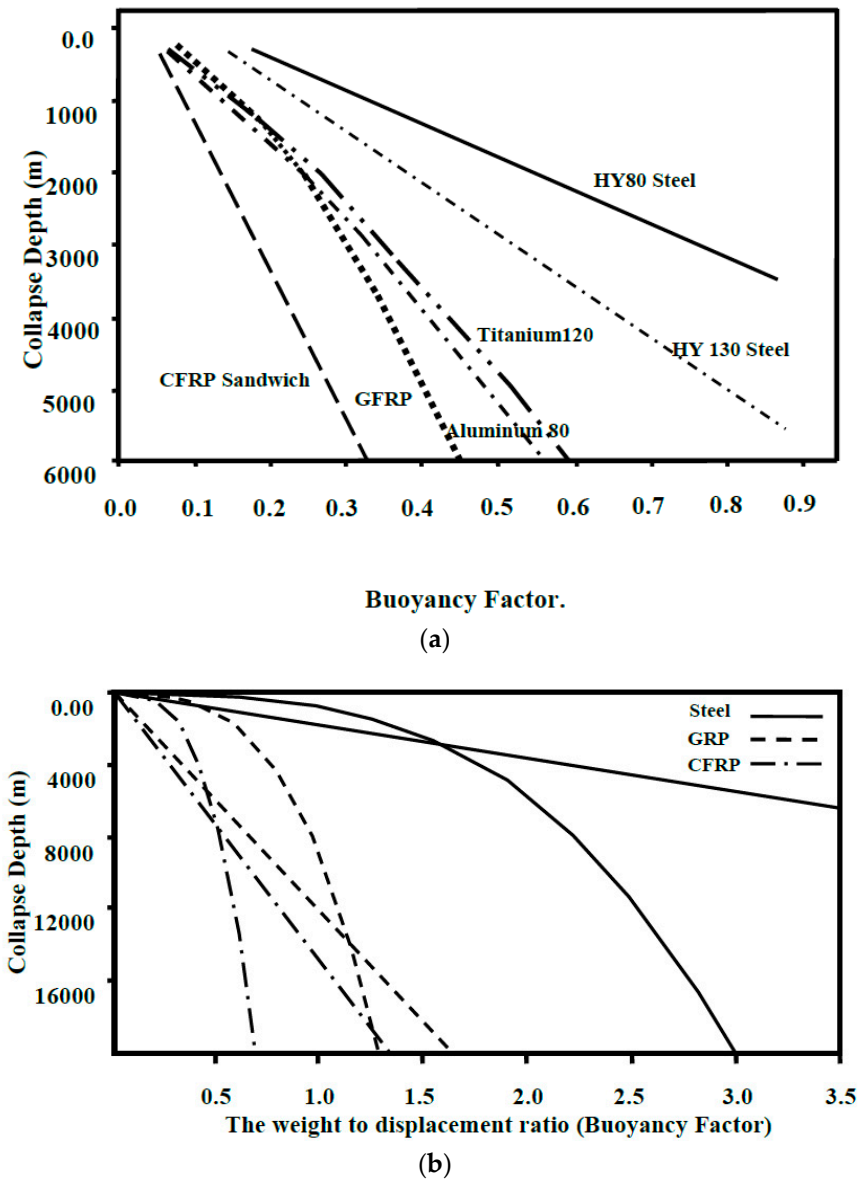

Figure 2. Weight to displacement ratio vs. collapse depth. (**a**) Weight to displacement ratio vs. Collapse depth for stiffened cylinders. (**b**) Weight to displacement ratio vs. collapse depth for un-stiffened cylinders.

5.1. Finite Element Modeling and Simulation of Composite Pressure Hull

Finite element modeling of sandwich composite hull was carryied out using ANSYS Parametric Design Language (APDL). The structure shell is modeled using SHELL281, which is suitable for analyzing thin to moderately thick shell structures. It is used for modeling composite shells or sandwich structure. The BEAM189 is used for the rings and long beams stiffeners [60,61]. Figure 3 demonstrates that the shell is consisting of a total 17 layers with stacking sequence $\left[(-\theta/\theta)_4/\overline{C}\right]_S$ including the core layer. The bottom layer designated as layer (1) and the additional layers were stacked from the bottom to the top. A symmetry boundary condition is applied in all nodes at (Y = 0 (X-Z plane) and X = 0 (Y-Z plane)) furthermore and due to the fluid flow in the longitudinal direction (Z-direction). One single node was constrained in the Z-direction as in [12,62]. The submarine in the vertical direction was balanced by the gravity and the buoyancy. Therefore, no restriction was imposed in the vertical direction. These boundary conditions permitted to capture a heave and pitch motion of submarine in the simulation. The pressure hull is loaded by external pressure ($P = \rho gH$) as a uniform external

pressure load. Where (ρ) is the density of sea water with a value of 1025 kg/m^3, (g) is the gravity acceleration which equals 9.81 m/s^2 and (H) is the depth below the water surface. If the hydrostatic pressure exceeds the critical values, the resultants of sandwich composite pressure hull shell element can introduce various failures. The mesh density greatly influences the optimization results; therefore, the mesh was selected as in [12]. Figure 4 shows the mesh for the model.

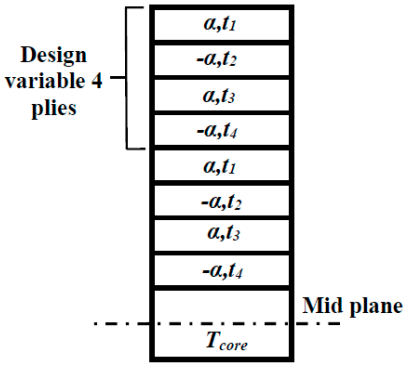

Figure 3. Design variables for the entire composite structure in a laminate.

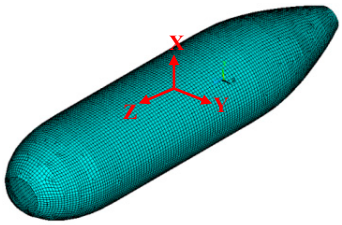

a) Shell element (SHELL281).

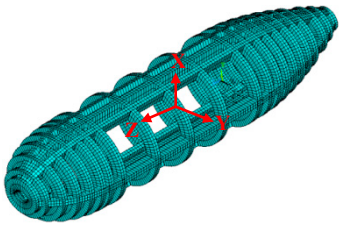

b) Beam element (BEAM189).

Figure 4. Mesh of global model.

5.2. Optimization Statement

Application of sandwich composite material introduces many design variables, since properties like material properties, orientation, and thickness for each individual layer must be specified throughout the structure. Furthermore, the analysis models are often large and many design criteria are present—such as mass, stiffness, and buckling [63–67]. The multi-objective optimization problem of sandwich composite hull under hydrostatic pressure was investigated to maximize the deck area, buckling strength factor and minimize buoyancy factor under constraints on failure strength, deflection of the sandwich composite shell. The parametric model of the sandwich composite hulls has to be built first. Thereafter, the objective function, constraints, and design variables were defined. The optimization procedures flow chart is presented in Figure 5. The random design generation method (RDGM), which is a sub type of the sub problem approximation used in (ANSYS) will be considered in this study. RDGM is a method of increasing accuracy and reducing the computational time.

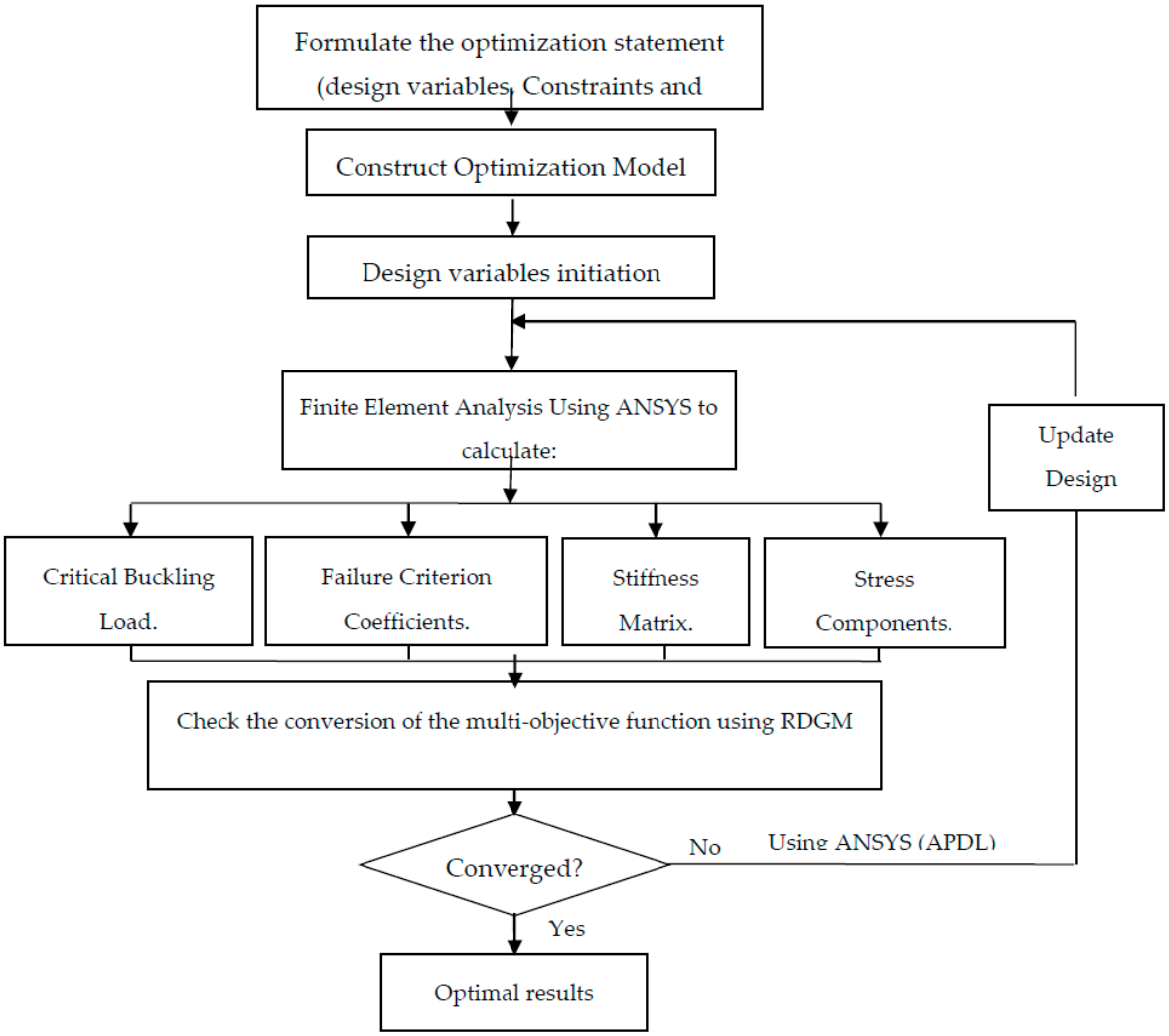

Figure 5. Optimization procedures.

5.3. Objectives of Optimization

The buoyancy factor (*B.F*) is defined as weight to buoyancy ratio (*W/B*) which is the most important factors related to the structural efficiencies of submarine pressure hull [68]. Moreover, the preliminary analysis of the deck area allows early assessment of arrangement feasibility. Therefore, it is assumed that maximizing the deck area is a target for execution the future arrangement. The optimization model of design includes the objective function, design constraints, and design variables. The multi-objective functions can be stated mathematically as shown in Equations (15)–(17).

$$\mathrm{F(X)}: \ \mathrm{Minimize} B.F = \frac{\text{Total hull weight}}{\text{The fluid displaced by the body volume.}} \tag{15}$$

$$\text{Maximize } A_{deck(tot)} = A_{deck(pmp)} + A_{deck(a)} + A_{deck(f)} \tag{16}$$

$$\text{Maximize buckling capacity}: \ \lambda = \frac{N_{cr}}{N_{act}} \tag{17}$$

5.4. Optimization Design Variables

In this study, the cross section radii of the sandwich composite pressure hull ((D_{min}) and (D_{max})), the thickness (t) of the individual layer, the thickness (T_{core}) of the core layer, and the fiber orientation

angle (α) of the individual layer are taken as design variables. For instance, the composite pressure hull diameters are taken as shown in Equation (18)

$$D_i^L \le D_i \le D_i^U, i = \max, \min \tag{18}$$

where D_i, D_i^L and D_i^U represent the ith sandwich composite pressure hull diameters, and its lower and upper limits, respectively. Similarly, the length of the main part is presented in Equation (19)

$$L_i^L \le L_i \le L_i^U, i = 1, 2, 3, 4 \tag{19}$$

where L_i, L_i^U and L_i^L represent the ith sandwich composite pressure hull length of the main part, and its upper and lower limits, respectively. Additionally, the core thickness is taken as shown in Equation (20)

$$T^L \le T_{core} \le T^U \tag{20}$$

where T_c, T^U and T^L represent the core thickness of the sandwich composite pressure hull, and its upper and lower limits, respectively. While the layer thickness is governed by Equation (21)

$$t^L \le t_i \le t^U, i = 1, 2, 3, \ldots, n \tag{21}$$

where t_i, t^L and t^U represent the i$^{\text{th}}$ thickness and the lower and upper bounds imposed on the individual layer thicknesses, respectively. On the other hand, the fiber orientation angle is presented as stated in Equation (22)

$$\alpha^{\mathrm{L}} \le \alpha_i \le \alpha^{\mathrm{U}}, \quad i = 1, 2, 3, \ldots, n \tag{22}$$

where α_i, α^L, and α^U represent the ith orientation angle of each layer and their upper and lower bounds, respectively. The zero-degree layer runs longitudinally in the submarine pressure hull.

5.5. Constraints of Optimization

Generally, the essential requirement that has to be satisfied in the design is the safety of structure under severe loading conditions. Tsai–Wu and maximum stress failure criteria were used in this study to judge the safety of the materials. Furthermore, (N_{cr}) is compared with the operating load (N) to ensure the buckling safety of structure. On the other hand, excessive deflections in shells and stiffeners could produce severe cracks and damage in the hull. Therefore, the maximum deflection value (δ) is compared with the maximum permissible deflection value ($\delta_{\max}$) for the sandwich composite pressure hull. The safety constraints are performed as follows:

5.5.1. Strength of Material Constraints

$$\mathrm{g}_1 : FI(i) - 1 \le 0, i = 1, 2, 3, \ldots\ldots n \tag{23}$$

where FI is the first-ply failure of angle-ply laminated for each i$^{\text{th}}$ layer and (n) is the number of layers.

$$\mathrm{g}_2 : \frac{\sigma}{\sigma_y} - 1 \le 0 \tag{24}$$

where σ and σ_y are the actual stress and yielding strength in the core layer, respectively.

5.5.2. Instability Constraint

$$\mathrm{g}_3 : \frac{N}{N_{cr}} - 1 \le 0 \tag{25}$$

where N_{cr} and N represent the minimum critical buckling load and the maximum actual operating loading, respectively, and calculated by ANSYS.

5.5.3. Maximum Operating Depth Constraint

$$g_4 : H \leq H_{\max} \tag{26}$$

where H and H_{max} represent the operating depth for the composite pressure hull and its maximum limits, respectively.

5.5.4. Maximum Deflection Value Constraint

$$g_5 : \delta \leq \delta_{\max} \tag{27}$$

where δ and $\delta_{\max}$ represent the deflection value for the composite pressure hull and its maximum permissible value, respectively.

6. Results

The optimization is performed for sandwich composite deep submarine pressure hull at extreme depths (up to 7500 m) using T700/Epoxy composite and shallow-to-moderate depths using B(4)5505/Epoxy. The achieved results were analyzed as follows:

6.1. At Extreme Depths

The results of the multi-objective optimization of sandwich composite hull constructed from T700/Epoxy are presented in Table 2. The multi-objective function (*MOF*), the (*B.F*), and (A_{deck}) are 0.48165, 0.60206, and 11.01364 m^2, respectively at maximum operating depth (H) equals 7500 m. While, the maximum deflection value (δ) and buckling strength factor (λ) are 26.873 mm and 47.902, respectively. Additionally, both Tsai–Wu (F_{TWSR}) and the maximum stress failure criteria (F_{MAXF}) are considered to predict the first-ply failure. The maximum values of (F_{TWSR} and F_{MAXF}) were 0.635 and 0.711, respectively which are occurred in the upper face at layer-17 due to high compression stresses. The optimized α is 53° with total half laminate thickens equals 52.04 mm. Figure 6 shows the (*FI*) for both maximum Tsai–Wu and maximum stress through the thickness. It was observed that the F_{MAXF} are slightly equal to F_{TWSR} and share the same trend. Based on the results obtained by carrying out the multi-objective optimization of sandwich composite submarine pressure hull at extreme depths, the upper and lower faces become thicker and the core thickness becomes thinner. These results are consistent with the results achieved by Liang [52].

Table 2. Results of the optimal design of sandwich composite pressure hull with T700/epoxy faces.

**	F_{TWSR}	F_{MAXF}	**	F_{TWSR}	F_{MAXF}	**Buckling Strength Factor (λ)**	**47.902**
FI-1	0.608	0.672	*FI-12*	0.596	0.663	t_1	3.821 (mm)
FI-2	0.5918	0.654	*FI-13*	0.620	0.690	t_2	6.502 (mm)
FI-3	0.6028	0.667	*FI-14*	0.602	0.672	t_3	7.276 (mm)
FI-4	0.582	0.644	*FI-15*	0.628	0.702	t_4	8.421 (mm)
FI-5	0.607	0.670	*FI-16*	0.611	0.684	α_1	53°
FI-6	0.584	0.64622	*FI-17*	0.635	0.711	T_{core}	14.009 (mm)
FI-7	0.609	0.67363	D_{max}	2.0055 (m)		LAY9_S_{XMAX}	3.48×10^6 Pa
FI-8	0.586	0.649	D_{min}	1.9675 (m)		LAY9_S_{XMIN}	-9.48×10^5 Pa
FI-10	0.593	0.659	Operating depth (H)	7500(m)		LAY9_S_{YMAX}	4.36×10^6 Pa
FI_11	0.618	0.686	Maximum deflection (δ_{MAX})	26.873 (mm)		LAY9_S_{YMIN}	-2.04×10^5 Pa
B.F	0.6028	-	A_{Deck}	11.01364(m^2)		*MOF*	0.48165

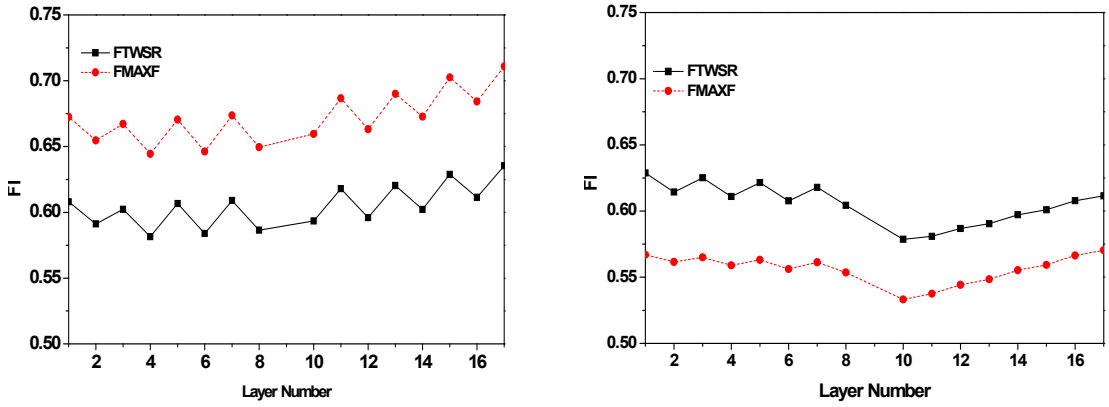

a) T700/epoxy composites at extreme depths. b) B(4)/5505 Boron/Epoxy at shallow depth.

Figure 6. Maximum Tsai–Wu and maximum stress failure index through the thickness.

6.2. At Shallow-to-Moderate Depths

The results of maximizing the buckling load capacity (λ) and minimizing ($B.F$) at shallow-to-moderate depths of the sandwich composite deep submarine pressure hull constructed from B(4)5505/Epoxy are summarized in Table 3. The buckling load capacity (λ), ($B.F$) and maximum deflection value (δ) are 118.80, 0.47, and 2.18 mm, respectively. The optimum configuration of the sandwich composite pressure hull can overcome all structural failures until operating depth (H) of up to 257.47 m. Furthermore, the maximum values of F_{TWSR} and F_{MAXF} are occurring in the lower face at layer-1 due to maximum tensile stresses with failure index (FI-1) of about 0.629 and 0.567, respectively. While, at upper face, the maximum values of F_{TWSR} and F_{MAXF} are occurring at layer-17 due to maximum compression stresses with failure index (FI-17) equals 0.611 and 0.570, respectively. The optimized orientation fiber α is equals (55°) with 90.71 mm (T_{core}). According to the aforementioned observations, it is safe to use sandwich composite pressure hull in submarines work at low to moderate depths.

Table 3. Results of the optimal design of sandwich composite pressure hull with B(4)/5505 Boron/Epoxy faces.

**	F_{TWSR}	F_{MAXF}	**	F_{TWSR}	F_{MAXF}	**Buckling Strength Factor (λ)**	**118.8**
FI-1	0.628	0.567	FI-12	0.586	0.544	t_1	1.59 (mm)
FI-2	0.614	0.561	FI-13	0.590	0.54846	t_2	1.59 (mm)
FI-3	0.625	0.565	FI-14	0.597	0.555	t_3	1.59 (mm)
FI-4	0.611	0.559	FI-15	0.600	0.559	t_4	1.59 (mm)
FI-5	0.621	0.563	FI-16	0.607	0.566	α_1	55°
FI-6	0.607	0.556	FI-17	0.611	0.570	T_{core}	97 (mm)
FI-7	0.617	0.561	D_{max}	2.0838(m)		$LAY9\_S_{XMAX}$	158772 Pa
FI-8	0.604	0.553	D_{min}	1.8842(m)		$LAY9\_S_{XMIN}$	−28654 Pa
FI-10	0.578	0.533	Operating depth (H)	257.47(m)		$LAY9\_S_{YMAX}$	219556.6 (Pa)
FI_11	0.581	0.537	Maximum deflection (δ_{MAX})	2.18 (mm)		$LAY9\_S_{YMIN}$	−69869 (Pa)
$B.F$	0.47077	-	-	-		MOF	0.00396

6.3. Effect of Fiber Orientation (α) on Design Variables and Constraints

Figure 7 presents the effect of α upon Tsai–Wu and maximum stress failure index for both upper and lower faces of sandwich composite hull. A number of interesting features were observed in this study. For instance, the Tsai–Wu and maximum stress failure indices are sensitive with (α). The maximum failure indices for both Tsai–Wu and maximum stress failures occur when (α = 0°). The maximum Tsai–Wu failure and maximum stress failure are 2.255 and 2.285, respectively and occur at (layer 1) due to the high tensile stresses in the lower face. On the other hand, at the upper face, F_{TWSR} and F_{MAXF} are 1.79 and 1.925, respectively and occur at the upper layer (layer 17) due to high compression stresses. As (α) increases, F_{TWSR} and F_{MAXF} decrease and acquire the lowest value at (α = 65°), for both the upper and lower faces. Conversely, as (α) increases up to 90°, the failure index also, increases. Figure 8a, demonstrates the effect of (α) on buckling strength factor (λ). The maximum buckling strength factor is 69 and occurs when α is between 55° and 60°. While, the minimum buckling strength factor is 8.5 and occurs at (α = 35°). Thereafter, with increasing (α), the buckling strength factor decreases and acquire its lowest value which is 10 when (α = 90°). Figure 8b shows the effect of (α) on maximum deflection values. The maximum and minimum deflection values are 0.058m and 0.018m, respectively. The minimum deflection value occurs when (α = 55°) while the maximum deflection occurs when (α = 0°). Based on the aforementioned observations, it can be concluded that the maximum buckling strength factor (λ) and minimum deflection values are achieved when (α) is between 55° and 60°. Furthermore, the fiber orientation (α) is highly related to buckling strength factor and deflection values.

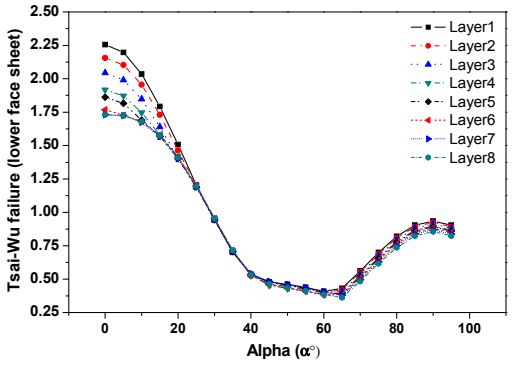

a) α vs. Tsai–Wu failure index (lower face sheet).

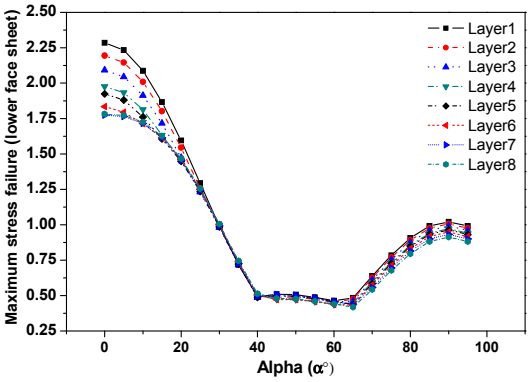

b) α vs. maximum stress failure index (lower face sheet).

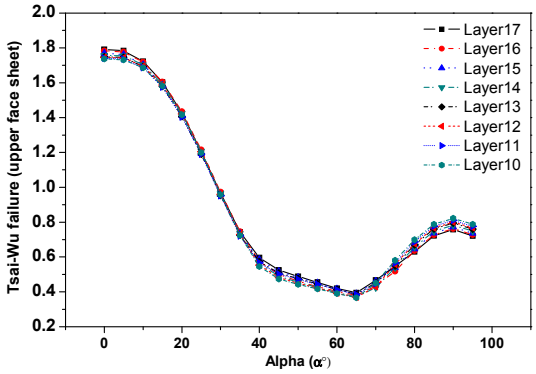

c) α vs. Tsai–Wu failure index (upper face sheet).

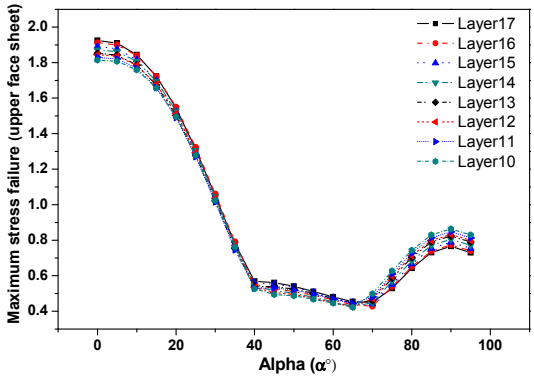

d) α vs. maximum stress failure index (upper face sheet).

Figure 7. Effect of fiber orientation (α) on the design variables and constraints.

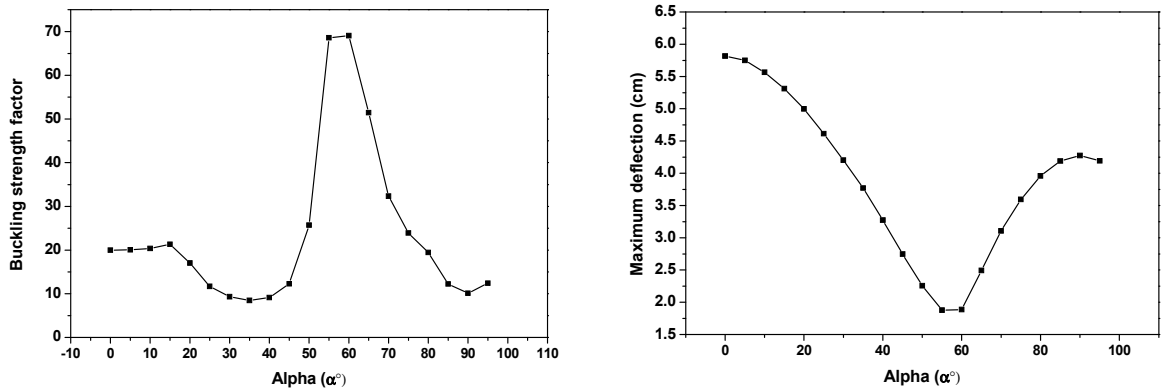

a) α vs. buckling strength factor. b) α vs. δ_{MAX}.

Figure 8. Effect of fiber orientation (α) on the buckling strength factor and maximum deflection value (δ_{MAX}).

6.4. Effect of Core Thickness (Tcore) on Design Variables and Constraints

Figure 9 shows the effect of core thickness (T_{core}) on both F_{TWSR} and F_{MAXF} at extreme depths. The core thickness varies from 0 to 280 mm. The sandwich treated here as a laminate where the core represents another layer with a thickness equals (T_{core}). From Figure 9a,b, it was observed that, F_{TWSR} and F_{MAXF} have the same trend. As (T_{core}) increases, the failure index of the lower face of sandwich composite pressure hull increases until (T_{core}) reaches up to 20 mm, after that as T_{core} exceeds this limit, the failure index of the lower face decreases. In addition, the results emphasize an important fact that, at extreme depths (T_{core}) has a little influence on both F_{TWSR} and F_{MAXF} at lower face. Figure 9c,d illustrates the effect of (T_{core}) on F_{TWSR} and F_{MAXF} of the upper face. As (T_{core}) increases, the failure index of the upper face increases until (T_{core}) reaches to 20 mm then, as T_{core} increases the failure index of the upper face decreases.

Figure 10 demonstrates the effect of (T_{core}) on F_{TWSR} and F_{MAXF} for the lower and upper faces for the sandwich composite deep submarine pressure hull, constructed from B(4)5505/Epoxy at low to moderate depths. It was revealed that, when (T_{core}) increases, the failure indices for both upper and lower faces of sandwich composite pressure hull are decrease. The obtained results emphasize that (T_{core}) has a major impact on Tsai–Wu and maximum stress failure indices for sandwich composite pressure hull at low to moderate depths. The aforementioned results emphasize an important fact that the presence of core layer in sandwich composite pressure hull is not always more efficient than the alternatives. Figure 11a shows the effect of (T_{core}) on the maximum deflection value for sandwich composite deep submarine pressure hull constructed from T700/Epoxy at different depths (7500 m, 8500 m, 9500 m, and 10,500 m). The figure illustrates that; the maximum deflection value is direct proportional to (T_{core}) when (T_{core}) ranges between 0 and 20 mm. Thereafter, the maximum deflection value is inversely proportional with increasing (T_{core}). In addition, the rate of changes of deflection values with (T_{core}) is small. Also, the figure demonstrates that increasing the operating depth increases the maximum deflection values with constant rate. Figure 11b depicts the effect of (T_{core}) on buckling strength factor at different depths (7500 m, 8500 m, 9500 m, and 10,500 m). The buckling strength factor is inversely proportional to (T_{core}) at the range of 0–20 mm. Then, as (T_{core}) increases, the buckling strength factor increases. The rate of changes of buckling strength factor with (T_{core}) is very small. The results obtained reveals that increasing the operating depths decreases the buckling strength factor with constant rate. Based on the above observations, the core thickness has a minor effect on both buckling strength factor and maximum deflection values at extreme depths. Figure 12a,b show the effect of (T_{core}) on maximum von Mises stresses and maximum compression shear stresses (S_{ZY}) in the core layer. The figures illustrate that increasing (T_{core}) decreases the maximum von Mises stresses and maximum compression shear stresses (S_{ZY}). Figure 12c,d demonstrate the effects of (T_{core}) on the maximum tensile stresses in both X and Y direction (S_{XMAX}) and (S_{YMAX}), respectively in the core

layer. It was observed that as (T_{core}) increases, the S_{XMAX} and S_{YMAX} increase until (T_{core}) up to 20 mm. Thereafter, when (T_{core}) increases by more than 20 mm, the S_{XMAX} and S_{YMAX} enhances with relatively small rate compared to that of (T_{core}). Figure 12e,f present the effects of (T_{core}) on maximum compression stresses in both X and Y direction (S_{XMIN}) and (S_{YMIN}), respectively, in the core layer. It was revealed that when (T_{core}) increases the S_{XMIN} and S_{YMIN} increase until (T_{core}) equals 20 mm. Then, when (T_{core}) increases by more than 20 mm, the values of S_{XMIN} and S_{YMIN} decrease with relatively small rate compared to that of the core thickness.

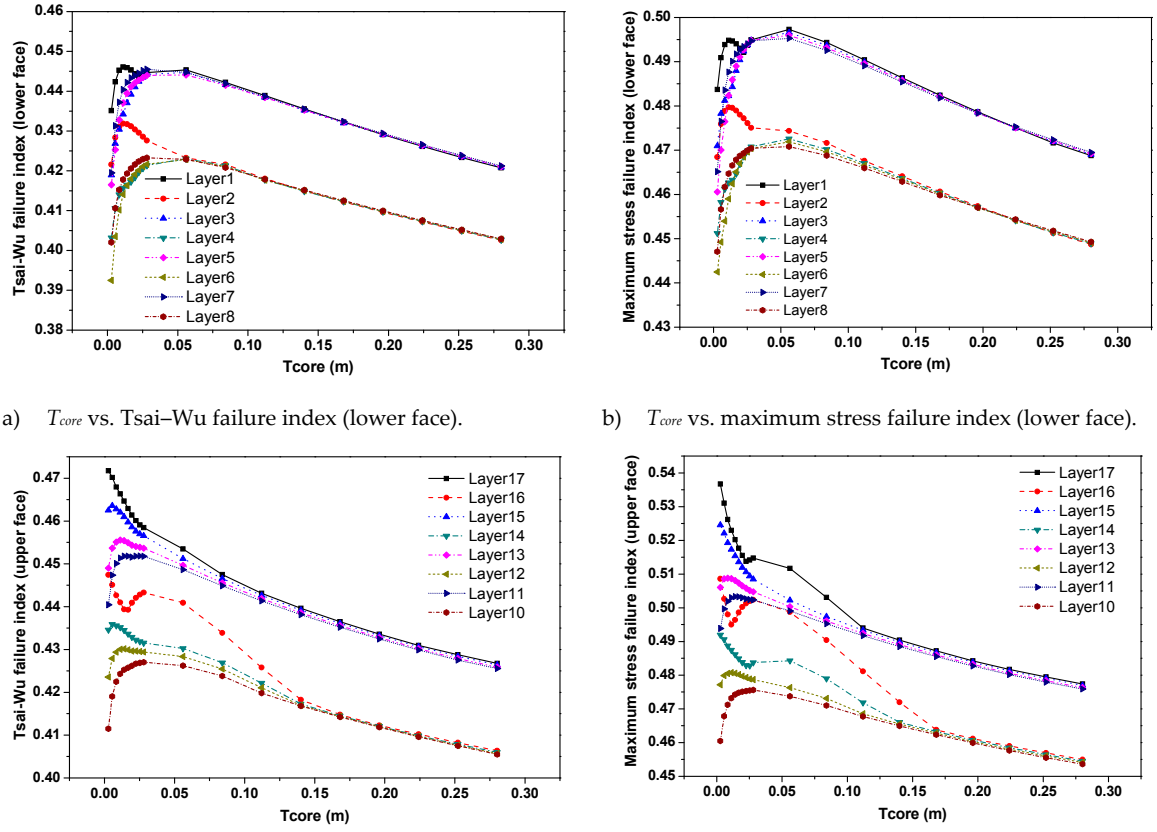

a) T_{core} vs. Tsai–Wu failure index (lower face).

b) T_{core} vs. maximum stress failure index (lower face).

c) T_{core} vs. Tsai–Wu failure index (upper face).

d) T_{core} vs. maximum stress failure index (upper face).

Figure 9. Effect of core thickness (T_{core}) on Tsai–Wu and maximum stress failure index at extreme depths.

6.5. Effect of Major Diameter (Dmax) and Minor Diameter (Dmin) on the Design Constraints

Figure 13a,b shows the variation of F_{TWSR} and F_{MAXF} on the lower face of the sandwich composite pressure hull with (D_{max}). When (D_{max}) increases, F_{TWSR} and F_{MAXF} for the lower face are decreased, especially when (D_{max}) and (D_{min}) about 1.95 m. Furthermore, the figures reveal that, the maximum F_{TWSR} and F_{MAXF} occur at the lower layer (layer 1) and the minimum F_{TWSR} and F_{MAXF} occurs at layer 8. Thereafter, upon increasing (D_{max}), F_{TWSR} and F_{MAXF} increase. Likewise, Figure 13c,d demonstrates the effect of (D_{max}) on the maximum Tsai–Wu and maximum stress failure for the upper face. It was observed that as (D_{max}) increases, the Tsai–Wu and maximum stress failure for the upper face decreases and achieve its minimum measurement at 1.95 m (D_{max}). Also, it was revealed that the maximum stress failure occurs at the upper layer (layer 17) and the minimum stress failure occurs at layer 10. Moreover, it was observed that the maximum F_{TWSR} and F_{MAXF} for the upper face are higher than the maximum F_{TWSR} and F_{MAXF} for the lower face. On the other hand, Figure 13e,g reflects the relationship between (D_{min}) and the failure index (FI) of both Tsai–Wu and maximum stress. It was observed that the (FI) in the upper face is higher than the lower face. Also, while (D_{min}) increases, the (FI) on the upper and lower faces decreases and acquire its minimum measurement when (D_{min}) equals (D_{max}).

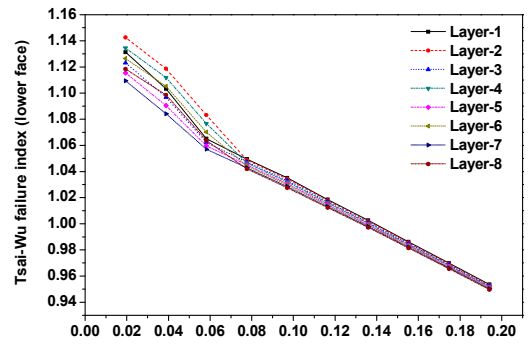

a) T_{core} vs. Tsai–Wu failure index (lower face).

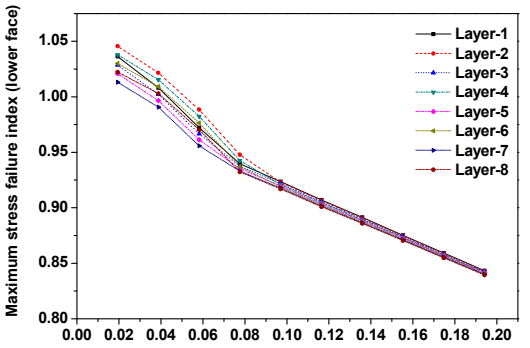

b) T_{core} vs. maximum stress failure index (lower face).

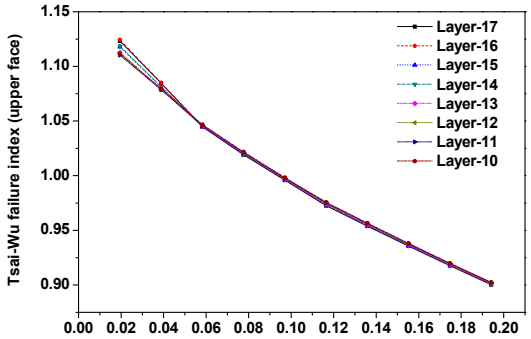

c) T_{core} vs. Tsai–Wu failure index (upper face).

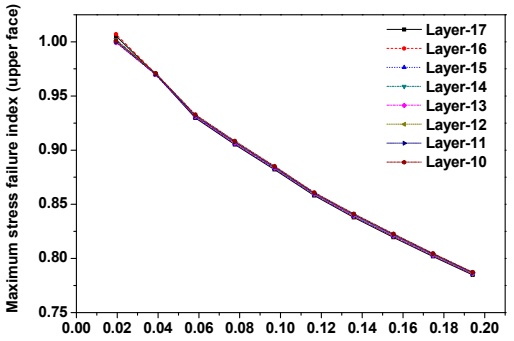

d) T_{core} vs. maximum stress failure index (upper face).

Figure 10. Effect of core thickness (T_{core}) on Tsai–Wu and maximum stress failure index at shallow depths.

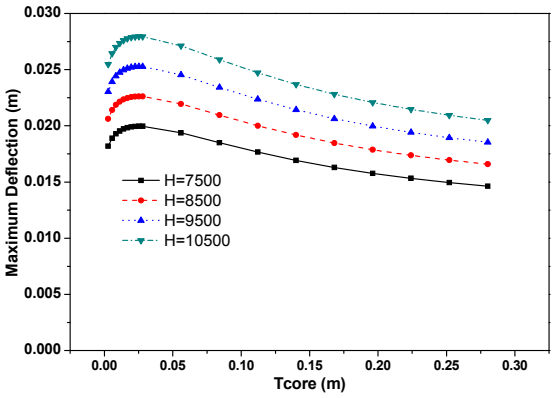

a) T_{core} vs. δ_{MAX}.

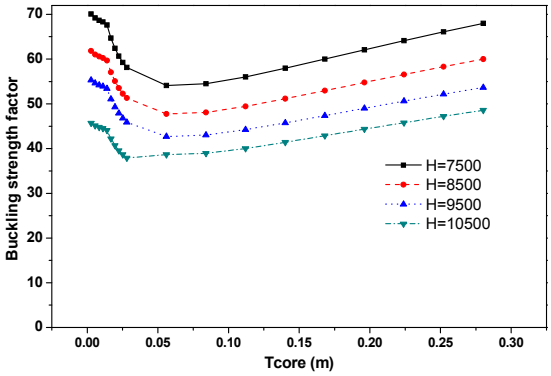

b) T_{core} vs. buckling strength factor.

Figure 11. Effect of T_{core} on the buckling strength factor and maximum deflection value (δ_{MAX}) at extreme depth.

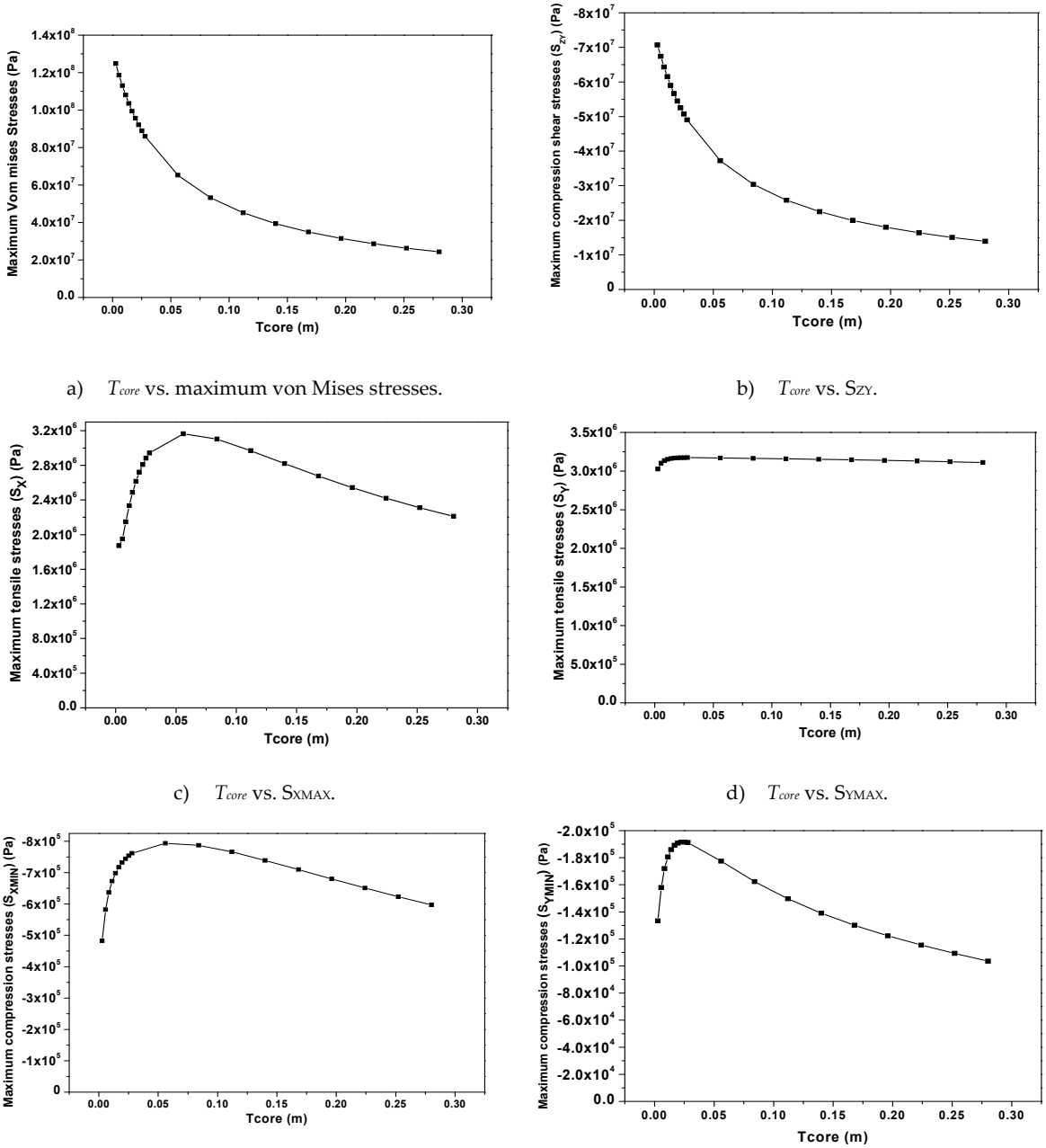

a) T_{core} vs. maximum von Mises stresses.

b) T_{core} vs. SZY.

c) T_{core} vs. SXMAX.

d) T_{core} vs. SYMAX.

e) T_{core} vs. SXMIN.

f) T_{core} vs. SYMIN.

Figure 12. Effect of T_{core} on the core layer stresses at extreme depth.

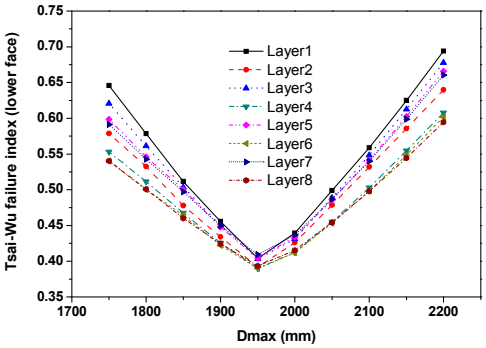

a) D_{max} vs. Tsai–Wu failure (lower face).

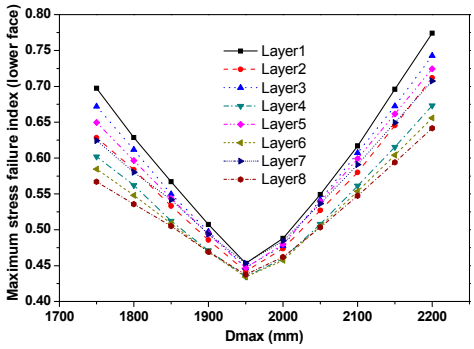

b) D_{max} vs. maximum stress failure (lower face).

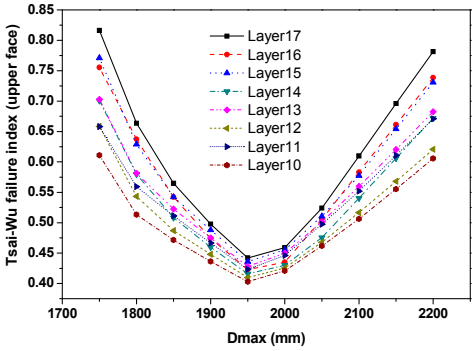

c) D_{max} vs. Tsai–Wu failure (upper face).

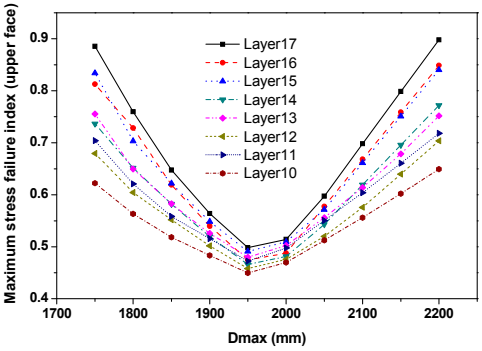

d) D_{max} vs. maximum stress failure (upper face).

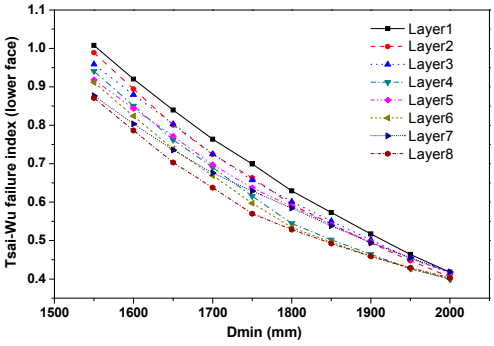

e) D_{min} vs. Tsai–Wu failure (lower face).

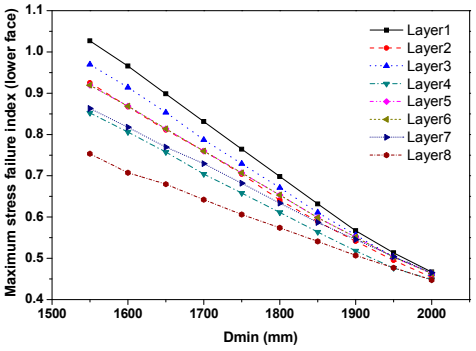

f) D_{min} vs. maximum stress failure (lower face).

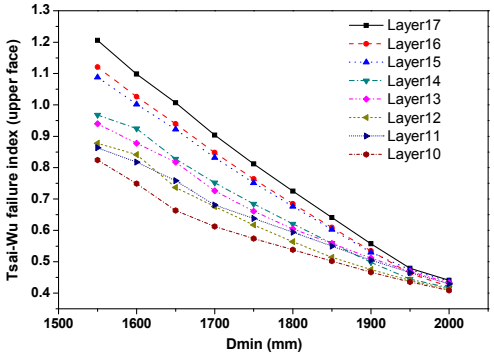

g) D_{min} vs. Tsai–Wu failure (upper face).

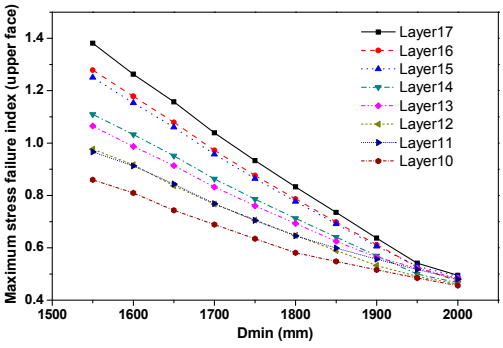

h) D_{min} vs. maximum stress failure (upper face).

Figure 13. Effect of (D_{max}) and (D_{min}) on Tsai–Wu and maximum stress failure at extreme depths.

7. Conclusions

Finite element simulation, sensitivity analysis, and optimization of sandwich composite deep submarine pressure hull were developed and presented in this study to minimize buoyancy factor and maximize deck area and buckling strength factor using two composite materials, T700/Epoxy and B(4)5505/Epoxy composite. The collapse depth is taken as a basis in the pressure hull calculations. Material failure, buckling, and deflection were considered.

Based on the aforementioned results, at extreme depths the thickness of the faces become thicker and the core thickness become thinner. The core thickness plays a minor role in the design of composite deep submarine pressure hull at extreme depths. Moreover, at extreme depths, the core thickness has a minor effect on Tsai–Wu, maximum stress failure coefficient, buckling strength factor, and maximum deflection measurements. Conversely, the laminated angle α has a major effect on Tsai–Wu, maximum stress failure coefficient, deflection value, and buckling strength factor. At extreme depths, the buckling strength factor becomes larger than the material failure. Therefore, the forces rather than the shell buckling were found to be the critical design consideration and the optimum design is governed by the material failure.

The presence of core layer in the sandwich composite pressure hull is not always more efficient. It depends on the geometry, loading, and design philosophy. At extreme depths, using monolithic laminates is recommended rather than the sandwich composite. Moreover, the use of sandwich is not a safe option in the event of possible damage to the external layer of the laminate in contact with sea water. However, at shallow-to-moderate depths, using the sandwich composite with a thick core is recommended to resist shell buckling. This research can also be used as a useful tool in the design of sandwich composite hulls of underwater vehicles.

Author Contributions: Conceptualization, E.F. and M.H.; Formal analysis, E.F.; Funding acquisition, D.W. and H.H.; Methodology, E.F.; Resources, E.F., M.H. and H.H.; Software, E.F. and M.H.; Supervision, E.F.; Writing–original draft, E.F.; Writing–review & editing, E.F. and M.H.

Funding: The authors are grateful for the support of this research by the 13th Five Years Key Programs for Science and Technology Development of China (Grant No. 2016YFD0701300), the Chinese Natural Science Foundation (Grant No. 51405076), and Heilongjiang Province Applied Technology Research and Development Program Major Project of China (Grant No. GA16B301). Also, the authors are grateful to Military Technical College (Cairo, Egypt), Taif University (Taif, KSA) and Mansoura University (Mansoura, Egypt) for providing all the required facilities to carry out the present research.

Acknowledgments: The authors are thankful to Military Technical College (Cairo-Egypt), Taif University (Taif-KSA) and Mansoura University (Mansoura-Egypt) for providing all the necessary facilities to carry out that research.

Conflicts of Interest: The authors declare no conflict of interest.

References

1. Pattison, D. *Design of Submarine Structures*; Defence Procurement Agency Sea Technology Group: Bristol, UK, 2001.
2. Davies, P. Behavior of Marine Composite Materials under Deep Submergence. In *Marine Applications of Advanced Fibre-Reinforced Composites*; Graham-Jones, J., Summerscales, J., Eds.; Woodhead Publishing: Sawston, Cambridge, UK, 2016; pp. 125–145.
3. Zhang, J.; Zhang, M.; Tang, W.; Wang, W.; Wang, M. Buckling of Spherical Shells Subjected to External Pressure: A Comparison of Experimental and Theoretical Data. *Thin-Walled Struct.* **2017**, *111*, 58–64. [CrossRef]
4. Zhang, M.; Tang, W.; Wang, F.; Zhang, J.; Cui, W.; Chen, Y. Buckling of Bi-Segment Spherical Shells under Hydrostatic External Pressure. *Thin-Walled Struct.* **2017**, *120*, 1–8. [CrossRef]
5. Naik, G.N.; Gopalakrishnan, S.; Ganguli, R. Design Optimization of Composites Using Genetic Algorithms and Failure Mechanism Based Failure Criterion. *Compos. Struct.* **2008**, *83*, 354–367. [CrossRef]
6. Mian, H.H.; Wang, G.; Dar, U.A.; Zhang, W. Optimization of Composite Material System and Lay-up to Achieve Minimum Weight Pressure Vessel. *Appl. Compos. Mater.* **2013**, *20*, 873–889. [CrossRef]

7. Helal, M.; Huang, H.; Fathallah, E.; Wang, D.; ElShafey, M.M.; Ali, M.A.E.M. Numerical Analysis and Dynamic Response of Optimized Composite Cross Elliptical Pressure Hull Subject to Non-Contact Underwater Blast Loading. *Appl. Sci.* **2019**, *9*, 3489. [CrossRef]
8. Pan, G.; Lu, J.; Shen, K.; Ke, J. *Optimization of Composite Cylindrical Shell Subjected to Hydrostatic Pressure*; Springer: Cham, Switzerland, 2015; pp. 81–90. [CrossRef]
9. Zhang, D.; Song, B.; Wang, P.; Chen, X. Multidisciplinary Optimization Design of a New Underwater Vehicle with Highly Efficient Gradient Calculation. *Struct. Multidiscip. Optim.* **2017**, *55*, 1483–1502. [CrossRef]
10. Pelletier, J.L.; Vel, S.S. Multi-Objective Optimization of Fiber Reinforced Composite Laminates for Strength, Stiffness and Minimal Mass. *Comput. Struct.* **2006**, *84*, 2065–2080. [CrossRef]
11. Lund, E. Discrete Material and Thickness Optimization of Laminated Composite Structures including Failure Criteria. *Struct. Multidiscip. Optim.* **2018**, *57*, 2357–2375. [CrossRef]
12. Fathallah, E.; Qi, H.; Tong, L.; Helal, M. Design Optimization of Lay-Up and Composite Material System to Achieve Minimum Buoyancy Factor for Composite Elliptical Submersible Pressure Hull. *Compos. Struct.* **2015**, *121*, 16–26. [CrossRef]
13. Fathallah, E.; Qi, H.; Tong, L.; Helal, M. Multi-Objective Optimization of Composite Elliptical Submersible Pressure Hull for Minimize the Buoyancy Factor and Maximize Buckling Load Capacity. *Appl. Mech. Mater.* **2014**, *578–579*, 75–82. [CrossRef]
14. Fathallah, E.; Qi, H.; Tong, L.; Helal, M. Design Optimization of Composite Elliptical Deep-Submersible Pressure Hull for Minimizing the Buoyancy Factor. *Adv. Mech. Eng.* **2014**, *6*, 987903. [CrossRef]
15. Fathallah, E. Finite Element Modelling and Multi-Objective Optimization of Composite Submarine Pressure Hull Subjected to Hydrostatic Pressure. *Mater. Sci. Forum* **2019**, *953*, 53–58. [CrossRef]
16. Panteleev, A.D. Optimal Design of Minimum Weight Sandwich Plates and Shallow Shells. *Appl. Mech.* **1984**, *20*, 103–107. [CrossRef]
17. Garland, C. Design and Fabrication of Deep-Diving Submersible Pressure Hulls. *SNAME Transactions* **1968**, *76*, 161–179.
18. Messager, T.; Pyrz, M.; Gineste, B.; Chauchot, P. Optimal Laminations of Thin Underwater Composite Cylindrical Vessels. *Compos. Struct.* **2002**, *58*, 529–537. [CrossRef]
19. Ca, B.; Liu, Y.; Liu, Z.; Tian, X.; Ji, R.; Li, H. Reliability-Based Load and Resistance Factor Design of Composite Pressure Vessel Under External Hydrostatic Pressure. *Compos. Struct.* **2011**, *93*, 2844–2852. [CrossRef]
20. Lee, G.C.; Kweon, J.H.; Choi, J.H. Optimization of Composite Sandwich Cylinders for Underwater Vehicle Application. *Compos. Struct.* **2013**, *96*, 691–697. [CrossRef]
21. Smith, M.J.; Macadam, T.; MacKay, J.R. Integrated Modelling, Design and Analysis of Submarine Structures. *Ships Offshore Struct.* **2015**, *10*, 349–366. [CrossRef]
22. Sekulski, Z. Multi-Objective Topology and Size Optimization of High-Speed Vehicle-Passenger Catamaran Structure by Genetic Algorithm. *Mar. Struct.* **2010**, *23*, 405–433. [CrossRef]
23. Aly, M.F.; Hamza, K.T.; Farag, M.M. A Materials Selection Procedure for Sandwiched Beams via Parametric Optimization with Applications in Automotive Industry. *Mater. Des.* **2014**, *56*, 219–226. [CrossRef]
24. Walker, M.; Smith, R.E. A Technique for the Multiobjective Optimisation of Laminated Composite Structures Using Genetic Algorithms and Finite Element Analysis. *Compos. Struct.* **2003**, *62*, 123–128. [CrossRef]
25. Akbulut, M.; Sonmez, F.O. Optimum Ddesign of Composite Laminates for Minimum Thickness. *Comput. Struct.* **2008**, *86*, 1974–1982. [CrossRef]
26. Bakshi, K.; Chakravorty, D. First Ply Failure Study of Thin Composite Conoidal Shells Subjected to uniformly Distributed Load. *Thin-Walled Struct.* **2014**, *76*, 1–7. [CrossRef]
27. Kalantari, M.; Dong, C.; Davies, I.J. Multi-Objective Robust Optimization of Multi-Directional Carbon/Glass Fibre-Reinforced Hybrid Composites with Manufacture Related Uncertainties under Flexural Loading. *Compos. Struct.* **2017**, *182*, 132–142. [CrossRef]
28. Liang, C.C.; Shiah, S.W.; Jen, C.Y.; Chen, H.W. Optimum Design of Multiple Intersecting Spheres Deep-Submerged Pressure Hull. *Ocean Eng.* **2004**, *31*, 177–199. [CrossRef]
29. Kim, T.U.; Shin, J.W.; Hwang, I.H. Stacking Sequence Design of a Composite Wing Under a Random Gust Using a Genetic Algorithm. *Comput. Struct.* **2007**, *85*, 579–585. [CrossRef]
30. MacKay, J.R.; Smith, M.J.; van Keulen, F.; Bosman, T.N.; Pegg, N.G. Experimental Investigation of the Strength and Stability of Submarine Pressure Hulls with and without Artificial Corrosion Damage. *Mar. Struct.* **2010**, *23*, 339–359. [CrossRef]

31. Zhang, J.; Wang, M.; Wang, W.; Tang, W.; Zhu, Y. Investigation on Egg-Shaped Pressure Hulls. *Mar. Struct.* **2017**, *52*, 50–66. [CrossRef]
32. Song, B.; Lyu, D.; Jiang, J. Optimization of Composite Ring Stiffened Cylindrical Hulls for Unmanned Underwater Vehicles Using Multi-Island Genetic Algorithm. *J. Reinf. Plast. Compos.* **2018**, *37*, 668–684. [CrossRef]
33. Carpentieri, G.; Skelton, R.E. On the Minimal Mass Design of Composite Membranes. *Compos. Part B Eng.* **2017**, *115*, 244–256. [CrossRef]
34. Ren, M.; Li, T.; Huang, Q.; Wang, B. Numerical Investigation into the Buckling Behavior of Advanced Grid Stiffened Composite Cylindrical Shell. *J. Reinf. Plast. Compos.* **2014**, *33*, 1508–1519. [CrossRef]
35. Rao, A.R.M.; Lakshmi, K. Optimal Design of Stiffened Laminate Composite Cylinder Using a Hybrid SFL Algorithm. *J. Compos. Mater.* **2012**, *46*, 3031–3055. [CrossRef]
36. Zhu, Y.; Ma, Q.; Zhang, J.; Tang, W.; Dai, Y. Opening Reinforcement Design and Buckling of Spherical Shell Subjected to External Pressure. *Int. J. Press. Vessel. Pip.* **2017**, *158*, 29–36. [CrossRef]
37. Ross, C.T.F.; Little, A.P.F. The Buckling of a Corrugated Carbon Fibre Cylinder Under External Hydrostatic Pressure. *Ocean Eng.* **2001**, *28*, 1247–1264. [CrossRef]
38. Lopatin, A.V.; Morozov, E.V. Buckling of Composite Cylindrical Shells with Rigid End Disks under Hydrostatic Pressure. *Compos. Struct.* **2017**, *173*, 136–143. [CrossRef]
39. Aydogdu, M.; Aksencer, T. Buckling of Cross-Ply Composite Plates with Linearly Varying In-Plane Loads. *Compos. Struct.* **2018**, *183*, 221–231. [CrossRef]
40. Han, J.Y.; Jung, H.Y.; Cho, J.R.; Choi, J.H.; Bae, W.B. Buckling Analysis and Test of Composite Shells under Hydrostatic Pressure. *J. Mater. Process. Technol.* **2008**, *201*, 742–745. [CrossRef]
41. Vosoughi, A.R.; Darabi, A.; Dehghani Forkhorji, H. Optimum Stacking Sequences of Thick Laminated Composite Plates for Maximizing Buckling Load Using FE-GAs-PSO. *Compos. Struct.* **2017**, *159*, 361–367. [CrossRef]
42. Erdal, O.; Sonmez, F.O. Optimum Design of Composite Laminates for Maximum Buckling Load Capacity Using Simulated Annealing. *Compos. Struct.* **2005**, *71*, 45–52. [CrossRef]
43. Vinson, J.R.; L, R. *The Behavior Of Structures Composed Of Composite Materials*; Springer: Dordrecht, The Netherlands, 2008. [CrossRef]
44. Ghasemi, A.R.; Hajmohammad, M.H. Multi-Objective Optimization of Laminated Composite Shells for Minimum Mass/Cost and Maximum Buckling Pressure with Failure Criteria under External Hydrostatic Pressure. *Struct. Multidiscip. Optim.* **2017**, *55*, 1051–1062. [CrossRef]
45. Kaw, A.K. *Mechanics of Composite Materials*, 2nd ed.; CRC Press Taylor & Francis Group: Boca Raton, FL, USA, 2006.
46. Li, B.; Pang, Y.-j.; Cheng, Y.-x.; Zhu, X.-m. Collaborative Optimization for Ring-Stiffened Composite Pressure Hull of Underwater Vehicle Based on Lamination Parameters. *Int. J. Nav. Archit. Ocean Eng.* **2017**, *9*, 373–381. [CrossRef]
47. Soden, P.D.; Hinton, M.J.; Kaddour, A.S. A Comparison of the Predictive Capabilities of Current Failure Theories for Composite Laminates. *Compos. Sci. Technol.* **1998**, *58*, 1225–1254. [CrossRef]
48. Barbero, E.J. *Finite Element Analysis of Composite Materials Using Abaqus*; CRC PressTaylor & Francis Group: Boca Raton, FL, USA, 2013.
49. Lopez, R.H.; Miguel, L.F.F.; Belo, I.M.; Cursi, J.E.S. Advantages of Employing a Full Characterization Method over Form in the Reliability Analysis of Laminated Composite Plates. *Compos. Struct.* **2014**, *107*, 635–642. [CrossRef]
50. Shrivastava, S.; Mohite, P.M.; Yadav, T.; Malagaudanavar, A. Multi-Objective Multi-Laminate Design and Optimization of a Carbon Fibre Composite Wing Torsion Box Using Evolutionary Algorithm. *Compos. Struct.* **2018**, *185*, 132–147. [CrossRef]
51. Tsai, S.W.; Wu, E.M. A General Theory of Strength for Anisotropic Materials. *J. Compos. Mater.* **1971**, *5*, 58–80. [CrossRef]
52. Liang, C.C.; Chen, H.W.; Jen, C.Y. Optimum Design of Filament-wound Multilayer Sandwich Submersible Pressure Hulls. *Ocean Eng.* **2003**, *30*, 1941–1967. [CrossRef]
53. Burche, R.; Rydill, J. *Concepts in Submarine Design*; Cambridge University Press: Cambridge, UK, 1995.
54. Vlahopoulos, N.; Hart, C.G. A Multidisciplinary Design Optimization Approach to Relating Affordability and Performance in a Conceptual Submarine. *J.Ship Prod.* **2010**, *26*, 273–289.

55. Ross, C.T.F. A Conceptual Design of an Underwater Missile Launcher. *Ocean Eng.* **2005**, *32*, 85–99. [CrossRef]
56. Fathallah, E.; Qi, H.; Tong, L.; Helal, M. Optimal Design Analysis of Composite Submersible Pressure Hull. *Appl. Mech. Mater.* **2014**, *578*, 89–96. [CrossRef]
57. Zheng, J.Y.; Liu, P.F. Elasto-Plastic Stress Analysis and Burst Strength Evaluation of Al-carbon Fiber/Epoxy Composite Cylindrical Laminates. *Comput. Mater. Sci.* **2008**, *42*, 453–461. [CrossRef]
58. Panahi, B.; Ghavanloo, E.; Daneshmand, F. Transient Response of a Submerged Cylindrical Foam Core Sandwich Panel Subjected to Shock Loading. *Mater. Des.* **2011**, *32*, 2611–2620. [CrossRef]
59. Smith, C.S. Design of Submersible Pressure Hulls in Composite Materials. *Mar. Struct.* **1991**, *4*, 141–182. [CrossRef]
60. Inc, A. *ANSYS Theory Reference Release 14.5*; ANSYS Inc.: Canonsburg, PA, USA, 2012.
61. Erdogan, M.; Ibrahim, G. *The Finite Element Method and Applications in Engineering Using ANSYS*; Springer: New York, NY, USA, 2006.
62. Ma, S.; Mahfuz, H. Finite Element Simulation of Composite Ship Structures with Fluid Structure Interaction. *Ocean Eng.* **2012**, *52*, 52–59. [CrossRef]
63. Lund, E. Buckling Topology Optimization of Laminated Multi-Material Composite Shell Structures. *Compos. Struct.* **2009**, *91*, 158–167. [CrossRef]
64. Sørensen, S.N.; Sørensen, R.; Lund, E. DMTO–A Method for Discrete Material and Thickness Optimization of Laminated Composite Structures. *Struct. Multidiscip. Optim.* **2014**, *50*, 25–47. [CrossRef]
65. Lindgaard, E.; Lund, E. Nonlinear Buckling Optimization of Composite Structures. *Comput. Methods Appl. Mech. Eng.* **2010**, *199*, 2319–2330. [CrossRef]
66. Lindgaard, E.; Lund, E.; Rasmussen, K. Nonlinear Buckling Optimization of Composite Structures Considering "worst" Shape Imperfections. *Int. J. Solids Struct.* **2010**, *47*, 3186–3202. [CrossRef]
67. Lindgaard, E.; Lund, E. A Unified Approach to Nonlinear Buckling Optimization of Composite Structures. *Comput. Struct.* **2011**, *89*, 357–370. [CrossRef]
68. Liu, T.; Xu, Q.; Chen, J.; Qian, M. Design of Submersible Vehicles in Sandwich Composites. In Proceedings of the 2000 International Symposium on Underwater Technology (Cat. No.00EX418), Tokyo, Japan, 26 May 2000; IEEE: Piscataway, NJ, USA, 2000; pp. 279–283.